Electronic Supplementary Material

Establishing plasmon contribution to chemical reactions: alkoxyamines as thermal probe

Olga Guselnikova [a], Gérard Audran[b], Jean-Patrick Joly[b], Andrii Trelin[c], Evgeny V. Tretyakov [d],[e], Vaclav Svorcik[c], Oleksiy Lyutakov[c], Sylvain R. A. Marque [b]*, Pavel Postnikov[a],[c]*

[a] Research School of Chemistry and Applied Biomedical Sciences, Tomsk Polytechnic University, Russian Federation;

[b] Aix-Marseille Univ, CNRS, ICR case 551, Avenue Escadrille Normandie-Niemen, 13397 Marseille Cedex 20, France;

[c] Department of Solid-State Engineering, University of Chemistry and Technology, Prague, Czech Republic;

[d] N.N. Vorozhtsov Novosibirsk Institute of Organic Chemistry, 9 Ac. Lavrentiev Avenue, Novosibirsk 630090, Russia;

[e] N.D. Zelinsky Institute of Organic Chemistry, Leninsky Prospect, 47, Moscow 119991, Russia

Table of Contents

Table of Content

Experimental Procedures

General

Solvents and reactants for the preparation of alkoxyamines **1** and **2** were used as received. Routine reaction monitoring was performed using silica gel 60 F254 TLC plates; spots were visualized upon exposure to UV light and a phosphomolybdic acid solution in EtOH, followed by heating. Purifications were performed on Reveleris® X2 Flash System BUCHI Switzerland on cartridges flash Reveleris® et GraceResolv™ : silica 40 μm weight (g). ^{1}H and ^{13}C NMR spectra were recorded in $CDCl_3$ on a 300 spectrometer. Chemical shifts (δ) in ppm were reported using residual non deuterated solvents as internal reference for ^{1}H and ^{13}C-NMR spectra. High-resolution mass spectra (HRMS) were performed on a SYNAPT G2 HDMS (Waters) spectrometer equipped with a pneumatically assisted atmospheric pressure ionization source (API). Positive mode electrospray ionization was used on samples: electrospray voltage (ISV): 2800 V; opening voltage (OR): 20 V; nebulizer gas pressure (nitrogen): 800 L/h. Low resolution mass spectra were recorded on the ion trap AB SCIEX 3200 QTRAP equipped with an electrospray source. The parent ion $[M+H]^+$ is quoted.

Preparation of AuNPs

Gold nanospheres were prepared by a modified Turkevich method [S1]. In 250 mL round bottomed flask, 1 mL of $HAuCl_4$ (100 mg in 10 mL) and 2.5 mL of Na_3CA (284.9 mg in 25 mL) were added to 100 mL of boiling water. Heating was continued for 10 min during which time the solution become red. After cooling to room temperature, the nanosphere solution was used as prepared.

Preparation of alkoxyamines

*4-(1-((2,2,6,6-tetramethylpiperidin-1-yl)oxy)ethyl)aniline (**1**).*

To a stirred solution of Salen ligand (515 mg, 1.92 mmol, 0.15 eq.) in *i*-PrOH (20 mL) was added $MnCl_2$ (379 mg, 1.92 mmol, 0.15 eq.) in an open flask. After 30 minutes of stirring at room temperature, a solution of *TEMPO* (2.0 g, 12.80 mmol, 1 eq.) and *4-vinylaniline* (1,7 g, 14.08 mmol, 1.1 eq.) in *i*-PrOH (20 mL) was added first, then solid $NaBH_4$ (1.3 g, 38.40 mmol, 3 eq.) in small portions. The resulting suspension was stirred at room temperature for 4h. It was then diluted with EtOAc (100 mL) and 1 M aq. HCl was carefully added. Solid $NaHCO_3$ was then added until neutralization. The layers were separated, and the organic phase was washed with water, brine and dried over $MgSO_4$. After concentration under reduced pressure, the residue was purified by column chromatography (petroleum ether/EtOAc; gradient: 100% to 50%) to afford the alkoxyamines ***1*** (1.8 g, 52%). Pale yellow solid; m.p.: 87°C (decomp.); ^{1}H NMR (300 MHz, $CDCl_3$) δ : 7.15 (d, *J* = 8.1 Hz, 2H), 6.66 (d, *J* = 8.1 Hz, 2H), 4.73 (q, *J* = 6.6 Hz, 1H), 3.61 (s, 2H), 1.49 (m, 9H), 1.30 (m, 3H), 1.20 (m, 3H), 1.07 (s, 3H), 0.73 (s, 3H). ^{13}C NMR (75 MHz, $CDCl_3$) δ : 144.8 (C), 135.6 (C), 127.5 (2 × CH), 114.4 (2 × CH), 82.2 (CH), 59.2 (C), 40.0 (2 × CH_2), 34.0 (2 × CH_3), 22.8 (CH_3), 20.0 (2 × CH_3), 16.9 (CH_2). HRMS *m/z* (ESI) Calcd for $C_{17}H_{29}N_2O^+$ $[M+H]^+$ 277.2274 Found: 277.2274.

*Diethyl (1-((1-(4-aminophenyl)ethoxy)(tert-butyl)amino)-2,2-dimethylpropyl)phosphonate (**2**)* was prepared according to [S2].

Diazotization and *in situ* modification

Modification of AuNPs with *in situ* generated diazonium was carried out in a mixture of water and methanol (1:1) at room temperature. To a solution of p-TsOH (0.019 g, 0.1 mmol) in methanol (2 mL), tert-butyl nitrite was slowly added (20 μL, 0.1 mmol). Next, the aniline derivative of an alkoxyamine initiator (0.05 mmol; 0.021 g for SG_1 and 0.14 g for TEMPO) was added in four steps to the reaction mixture during 1 min. The mixture was left to react for ~1.5 h prior to the functionalization. After 2 ml of water was added to the reaction mixture, it was incubated for 10 min. After that, 40 ml of as prepared AuNPs was added and stirred for 1 h. Next, the AuNPs were purified by

centrifugation (7500 rpm, 15 min) and washing with ethanol three times. The resulting AuNPs were resuspended in 5 ml of tert-butyl toluene. The prepared modified AuNPs were designated as Au-SG1 and Au-TEMPO.
To prepare the mixed conjugate (**Au-SG$_1$-TEMPO**), 0.01 g for SG1 and 0.07 g for TEMPO aniline derivatives were diazotized *in situ*, and 40 ml of as prepared AuNPs was added and stirred for 1 h. Then, the AuNPs were purified by centrifugation (7500 rpm, 15 min) and washing with ethanol three times. The resultant AuNPs were resuspended in 5 ml of tert-butyl toluene. The prepared modified AuNPs were designated as **Au-TEMPO-SG$_1$**.

Irradiation

A suspension of modified AuNPs (0.2 ml) was placed into an NMR tube, treated with ultrasound, and irradiated at a 1 cm distance with a LED (780 nm, 7 mW/mm^2; Thorlabs) from bottom to top. For kinetic measurements, the NMR tube was removed from the irradiation device and placed into an EPR cavity thermostated at 25 °C. Then, EPR spectra were recorded, and the NMR tube was removed from the EPR instrument and again irradiated by the LED under the same conditions, for various periods. Intensity of the LED irradiation was measured by Integrating Sphere Photodiode Power Sensors (Thorlabs, S142C).

Control experiments

A suspension of modified AuNPs (0.2 ml) was placed into an NMR tube, treated with ultrasound, and irradiated at a 1 cm distance with a LED (340 nm, 2 mW/mm^2; Thorlabs) or covered by foil and did not irradiated. All other measurements were performed as described above.

Analytical techniques

UV-Vis spectra were acquired on Spectrometer Lambda 25 (Perkin-Elmer) in the 300–1000 nm wavelength range. Raman scattering was measured on a portable ProRaman-L spectrometer at a 785 nm excitation wavelength (laser power 40 mW, integrations 100, average 1). Transmission electron micrographs of the nanoparticles were obtained by means of a JEOL JEM-1010 instrument operated at 80 kV (JEOL Ltd., Japan). EPR spectra were recorded on X-band ERD100 machines with the following parameters: modulation amplitude, 2G; gain, 105; sweep width, 200G; time constant, 50 ms; sweep time, 50 s; power, 10 mW. Intensity of the LED irradiation was measured by Integrating Sphere Photodiode Power Sensors (Thorlabs, S142C). Gold concentration was acquired on Flame Atomic Absorption Spectrometer Agilent 280FS AA with the measurement error 0-10%. Elemental organic analysis was performed on Vario EL Cube (Elementar GmbH).

Calculations of the local heating

The calculation was performed in the framework of Generalized Multiparticle Mie theory, implemented in the py_gmm software [S3]. The calculation was performed in the framework of Generalized Multiparticle Mie theory, implemented in the py_gmm software [S3].
For the calculation, following parameters were used:
Size of AuNPs: 13.5±2.1 nm
solvent: *tert*-buytl benzene
LED (780 nm) power 7 mW/mm^2 (Intensity of LED irradiation was measured by Integrating Sphere Photodiode Power Sensors (Throrlabs, S142C).

Table S1. Raman peaks assignments for Au-TEMPO and Au-SG1 (peaks assignation was made based on [S4, S5])

Raman peak frequencies (cm^{-1})	Assignments of peaks
Au-SG1	
1598	Ar ring str
1551	Ar ring str
1311	N-O vib
1271	P=O str
1162	C-N str
1182	C-N str
1043	Alk vib
986	Ar C-H def
877	Ar C-H def, Alk vib
771	Alk vib
568	Ar C=C def
473	Ar C=C def
382	Au-C str
Au-TEMPO	
1598	Ar ring str
1548	Ar ring str
1364	N-O vib
1309	C-N str
1150	C-N str
1035	Alk vib
986	Alk vib
760	Alk vib
680	Ar C=C def
567	Ar C=C def
472	Ar C=C def
393	Au-C str

Supplementary note 1. Description of experimental setup (Fig. 3)

For the plasmon-induced homolysis, the 0.5 ml NMR tube (sodium silicate glass outer diameter 5 mm, 18 cm height) was filled by the 0.2 ml of AuNPs suspensions (**Au-TEMPO**, **Au-SG$_1$**, **Au-SG$_1$-TEMPO**, **Au-SG$_1$**+**Au-TEMPO**) in tert-butylbenzene, actively treated in ultrasound bath for 15 minutes (25 kHz) and sealed with rubber coat. After, LED source (780 nm, ThorLab, product number M780LP1) was set up vertically to be the distance from LED to vial 1 cm. The spot size of LED was approximately 1 cm^2 (emitter diameter 3 mm) at this distance the power was measured 7 mW/mm^2 by Integrating Sphere Photodiode Power Sensors (Thorlabs, S142C). The sample was irradiated for a definite time period, subjected to EPR measurement. After sample was treated with the ultrasound and further illuminated. This procedure was repeated multiple times to get the kinetic data of plasmon-induced homolysis.

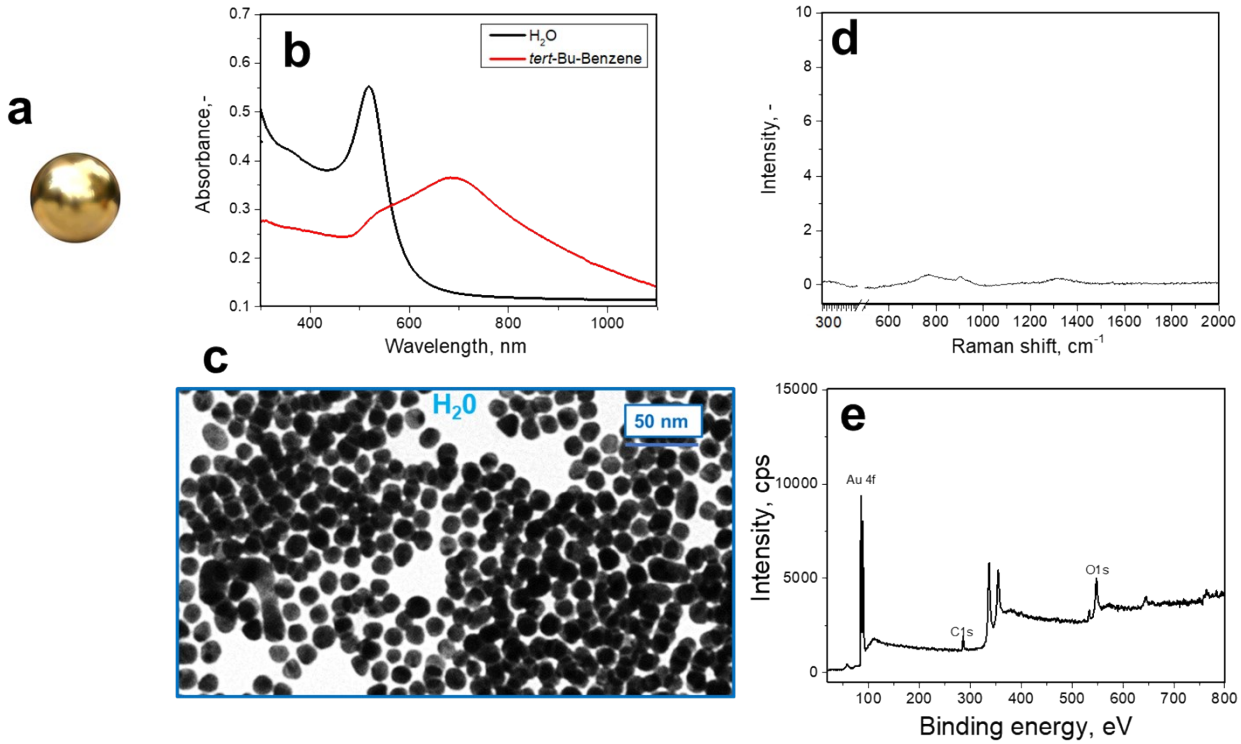

Figure S1. Detailed characterization of AuNPs (a) structure, (b) UV Vis spectra in water and tert-butylbenzene, (c) TEM image, (e) XPS survey spectra

Supplementary note 2. Characterization of AuNPs

As a starting material, we utilized AuNPs prepared by Turkevich method [S1]. As prepared AuNPs demonstrate the peak of plasmon resonance at 530 nm in water. In order to track changes of optical properties in the solvents used for EPR measurements – tert-butylbenzene, we centrifugated 40 ml AuNPs aqueous solution and washed it twice with ethanol, twice with tert-butylbenzene and the final volume of organic solvent was 3 ml. UV-Vis spectra in tert-butylbenzene demonstrate the wide peak (half with 250 nm) at ≈ 690 nm. According to TEM images, AuNPs demonstrated the average size 13.5 ± 2.1 nm (Fig. S1c). Transfer of AuNPs to tert-butylbenzene lead to the broadening of plasmon peak connected with the agglomeration or backscattering of AuNPs. XPS survey spectra revealed the Au, C and O on the surface due to the presence of citrate agent. SERS measured with 780 nm wavelength laser (40 mW, integrations 100, average 1) spectra does not demonstrate any significant peaks.

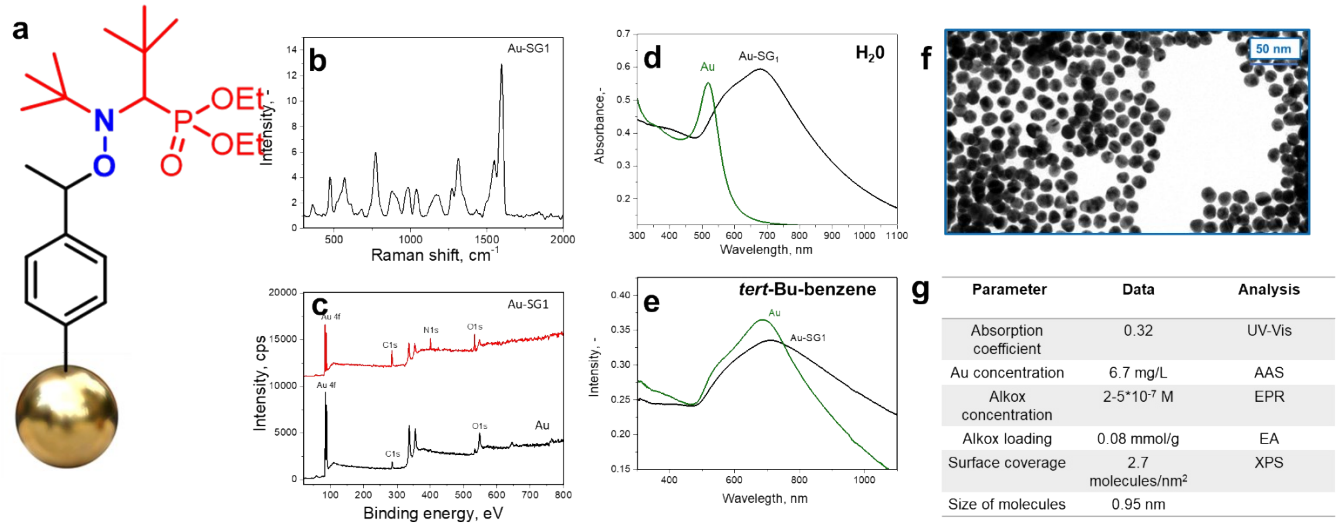

Parameter	Data	Analysis
Absorption coefficient	0.32	UV-Vis
Au concentration	6.7 mg/L	AAS
Alkox concentration	2-5*10^{-7} M	EPR
Alkox loading	0.08 mmol/g	EA
Surface coverage	2.7 molecules/nm^2	XPS
Size of molecules	0.95 nm	

Figure S2. Detailed characterization of **Au-SG$_1$** (a) structure, (b) SERS spectra , (c) XPS survey spectra, (d) UV-Vis spectra in water, (e) UV-Vis spectra in tert-butylbenzene (f) TEM image, (g) Summary table of parameters

*Supplementary note 3. Characterization of **Au-SG$_1$***

Au-SG$_1$ (Fig. S2a) were prepared by the diazotation of corresponding amine **(1)** in methanol followed by *in situ* modification by addition of 40 ml of AuNPs aqueous suspension and mixing with magnetic stirrer for 1 hour. After, **Au-SG$_1$** were separated and washed by centrifugation (7800 rpm, 10 min each cycle) with methanol and tert-butylbenzene;the final volume was 3 ml (tert-butylbenzene). SERS spectra (Fig. S2b) demonstrate the appearance of characteristic for alkoxyamine **(1)** peaks of aromatic ring, P=O stretch, C-N stretch and alkyl vibrations in the region 300-1700 cm^{-1} (see Tab. S1 for details). The peak at ≈380 cm^{-1} demonstrate the presence of Au-C covalent bonding [S4, S5]. XPS spectra revealed an increase in C1s (284.8 eV), O1s (532.7 eV), and N1s (400 eV) simultaneously with a decrease in the Au 4f (85.2–88.8 eV) peak intensities due to the covalent attachment of the organic moieties and screening of gold surface (Fig. S2c), the calculated thickness of organic layer is ≈1.8 nm. A photoemission spectrum of the N(1s) line is shown in Fig. S6, where the peaks ascribed to N–O bonds are detected similarly to those observed earlier [S4, S5] for SG1 moieties grafted on surfaces. UV-Vis measurment in water demonstrate the broadening and shift of peak – maximum ≈690 nm (half with 190 nm) (Fig. S2d). Transfer of **Au-SG$_1$** to tert-butylbenzene lead to the apperance of wider peak on UV-Vis spectra at 715 nm (half with 210 nm) (Fig. S2e). The observed broadening can be explained by the approaching of AuNPs to each other and some agregation (Fig. S2f), a dominant dipole feature is observed that is pushed into the infrared due to interparticle coupling or increased light scattering [S6, S7]. We also demonstrate the basic parameter of **Au-SG$_1$** suspension in tert-butylbenzene utilized for the furtther EPR study (Fig. S2g)- 0.2 ml was taken for the each experiment from 3 ml suspension. Absorption coefficient of suspension was used as a common unit used to quantify the concentration of AuNPs – 0.32. We also established the concentration of gold by atomic absorbtion spectroscopy (AAS), which was found to be 6.7 mg/L.

For the calculation of alkoxyamine loading three methods were uzed: EA, XPS-derived surface coverage calculated from the thickness of organic film and EPR measurment – after the plateu establishment of radical release. The change in nitrogen content after modification was used to calculate the alkox loading in mmol per g of AuNPs. The elemental composition of the grafted alkox SG$_1$ groups allowed us to establish 0.08 mmol of functional groups per 1 g of AuNPs. XPS calculation using the attenuation of Au peak enable us to detemine 2.7 molecules per nm^2, and EPR measurment reports a concentration of 2-5 *10 $^{-7}$ M. Using the AAS data and loading established by EA, it can be conlcuded the perfect covergence with EPR data.

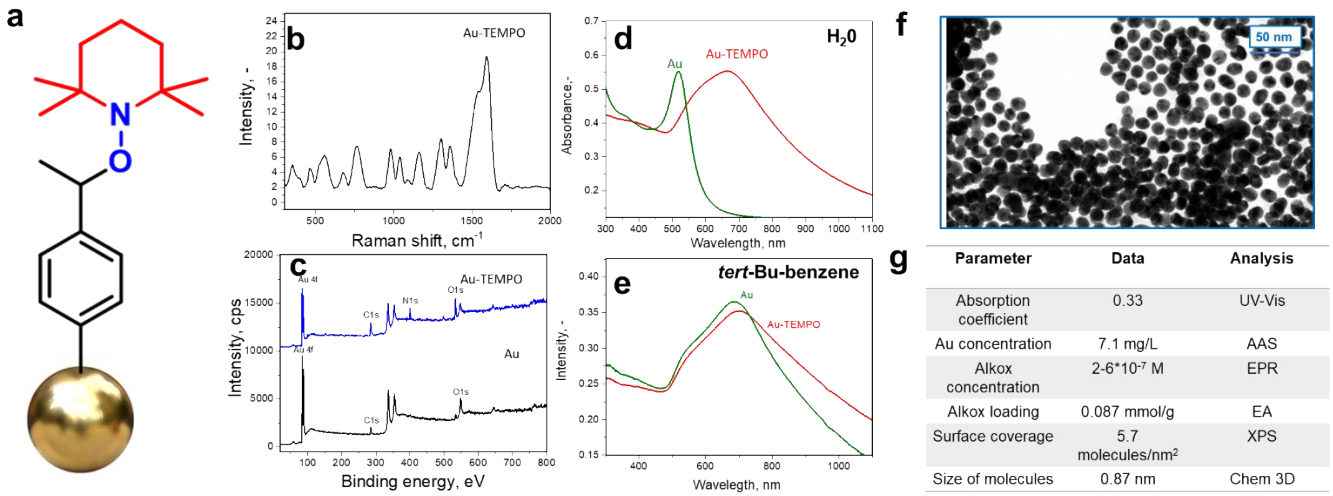

g

Parameter	Data	Analysis
Absorption coefficient	0.33	UV-Vis
Au concentration	7.1 mg/L	AAS
Alkox concentration	2-6*10^{-7} M	EPR
Alkox loading	0.087 mmol/g	EA
Surface coverage	5.7 molecules/nm^2	XPS
Size of molecules	0.87 nm	Chem 3D

Figure S3. Detailed characterization of **Au-TEMPO** (a) structure, (b) SERS spectra, (c) XPS survey spectra, (d) UV-Vis spectra in water, (e) UV-Vis spectra in tert-butylbenzene (f) TEM image, (g) Summary table of parameters

*Supplementary note 4. Characterization of **Au-TEMPO***

Au-TEMPO (Fig. S3a) were prepared by the diazotation of corresponding amine **(2)** in methanol followed by *in situ* modification by addition of 40 ml of AuNPs aqueous suspension and mixing with magnetic stirrer for 1 hour. After, **Au-TEMPO** were separated and washed by centrifugation (7800 rpm, 10 mon each cycle) with methanol and tert-butylbenzene; the final volume was 3 ml (tert-butylbenzene). SERS spectra (Fig. S3b) demonstrate the appearance of characteristic for alkoxyamine **(2)** peaks of aromatic ring, C-N stretch and alkyl vibrations in the region 300 -1700 cm^{-1} (see Tab. S1 for details). The peak at ≈390 cm^{-1} demonstrate the presence of Au-C covalent bonding [S4, S5]. XPS spectra (Fig. S3c) revealed an increase in C1s (284.8 eV), O1s (532.7 eV), and N1s (400 eV) simultaneously with a decrease in the Au 4f (85.2–88.8 eV) peak intensities due to the attachment of the organic moieties and screening of gold surface (Fig. S3c), the calculated thickness of organic layer is ≈2.1 nm. A photoemission spectrum of the N(1s) line is shown in Fig. S6, where the peaks ascribed to N–O bonds are detected similarly to those observed earlier [S4, S5] for TEMPO moieties grafted on surfaces. UV-Vis measurment in water demonstrate the broadening and shift of peak – maximum ≈675 nm (half with 195 nm) (Fig. S3d). Transfer of Au-TEMPO to tert-butylbenzene lead to the apperance of wider peak on UV-Vis spectra at 705 nm (half with 240 nm) (Fig. S3e, g). We also demonstrate the basic parameter (Fig. S3g) of Au-TEMPO suspension in tert-butylbenzene utilized for the furtther EPR study - 0.2 ml was taken for the each experiment from 3 ml suspension . Absorption coefficient of suspension was used as a common unit used to quantify the concentration of AuNps – 0.33. We also established the concentration of gold by atomic absorbtion spectroscopy (AAS), which was found to be 7.1 mg /L.

For the calculation of alkoxyamine loading three methods were uzed: EA, XPS-derived surface coverage calculated from the thickness of organic film and EPR measurment – after the plateu establishment of radical release. The change in nitrogen content after modification was used to calculate the alkox loading in mmol per g of AuNPs. The elemental composition of the grafted alkox SG-1 groups allowed us to establish 0.087 mmol of functional groups per 1 g of AuNPs. XPS calculation using the attenuation of Au peak enable us to detemine 5.7 molecules per nm^2, and EPR measurment reports a concentration of 2-6 *10 $^{-7}$ M. Using the AAS data and loading established by EA , it can be concluded the perfect covergence with EPR data.
Comparison of basic paramaters of **Au-SG$_1$** and **Au-TEMPO** (Fig. S2,3f) does not demosntarte the considerable difference in the basic paramaters descirbed in FigS2-3g, all deviation are with the one order of measured. The broadening of plasmonic peak of AuNPs appear to be alsmot identical, so these parameters (probable

agglomeration and scattering of AuNPs, amount of grafted alkoxyamine) can be neglected for the evaluation of plasmonic behaviour.

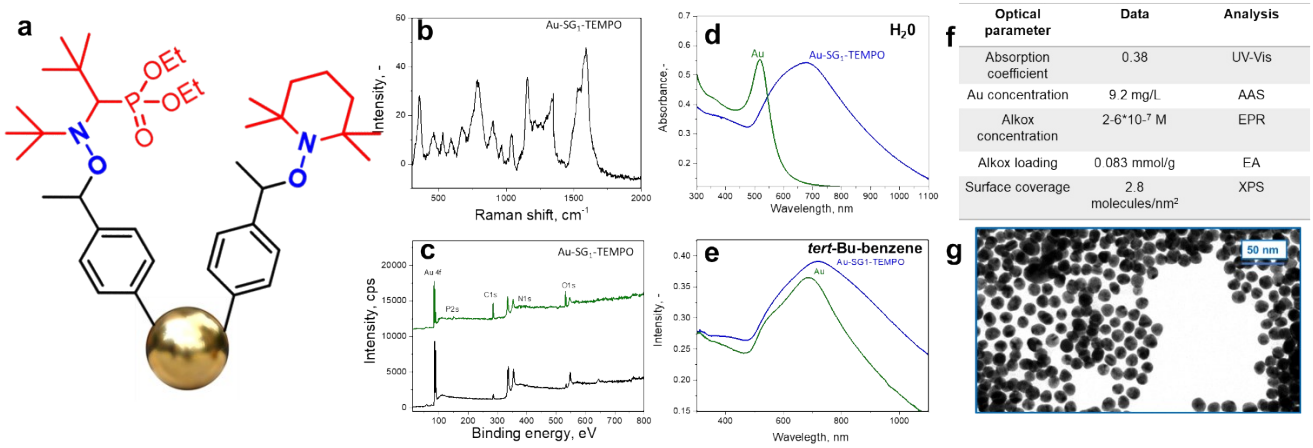

Figure S4. Detailed characterization of **Au-SG$_1$-TEMPO** (a) structure, (b) SERS spectra, (c) XPS survey spectra, (d) UV Vis spectra in water, (e) UV-Vis spectra in tert-butylbenzene (f) TEM image, (g) Summary table of parameters

*Supplementary note 5. Characterization of **Au-SG$_1$-TEMPO***

Au-SG$_1$-TEMPO (Fig. S4a) were prepared by the separate diazotation of corresponding amines **(1)** and **(2)** in methanol followed by their mixing and *in situ* modification by addition of 40 ml of AuNPs aqueous suspension and mixing with magnetic stirrer for 1 hour. After, **Au-SG$_1$-TEMPO** were separated and washed by centrifugation (7800 rpm, 10 min each cycle) with methanol and tert-butylbenzene; the final volume was 3 ml (tert-butylbenzene). SERS spectra (Fig. S4b) demonstrate the appearance of characteristic for alkoxyamines **(1)** and **(2)** peaks of aromatic ring, P=O stretch, C-N stretch and alkyl vibrations in the region 300 -1700 cm^{-1} (see Tab. S1 for details.). The position of peaks is almost identical as in case of separate grafting of alkoxyamines **(1)** and **(2)**. XPS spectra (Fig. S4c) revealed an increase in C1s (284.8 eV), O1s (532.7 eV), and N1s (400 eV) simultaneously with a decrease in the Au 4f (85.2–88.8 eV) peak intensities because of the attachment of the organic moieties and screening of gold surface (Fig. 1D, S1A), the calculated thickness of organic layer is ≈1.4 nm. The concentration of P as a marker element of SG1 enables the calculation of the ratio between TEMPO and SG$_1$, which was found to be 2.5:1. UV-Vis measurment in water demonstrate the broadening and shift of peak – maximum ≈695 nm (half with 200 nm) (Fig. S4d). Transfer of **Au-SG$_1$-TEMPO** to tert-butylbenzene lead to the apperance of wider peak on UV-Vis spectra at 720 nm (half with 270 nm) (Fig. S4e, f). We also demonstrate the basic parameter of Au-SG$_1$-TEMPO (Fig. S4g) suspension in tert-butylbenzene utilized for the furtther EPR study- 0.2 ml was taken for the each experiment from 3 ml suspension . Absorption coefficient of suspension wqas used as a common unit used to quantify the concentration of AuNPs – 0.38. We also established the concentration of gold by atomic absorbtion spectroscopy (AAS), which was found to be 9.2 mg /L.

For the calculation of alkoxyamine loading three methods were uzed: EA, XPS-derived surface coverage calculated from the thickness of organic film and EPR measurment – after the plateu establishment of radical release. The change in nitrogen content after modification was used to calculate the alkox loading in mmol per g of AuNPs. The elemental composition of the grafted alkox SG$_1$ groups allowed us to establish 0.083 mmol (total for both SG$_1$ and TEMPO, taking into account ratio TEMPO/SG$_1$= 2.5:1 from XPS) of functional groups per 1 g of AuNPs. XPS calculation using the attenuation of Au peak enable us to detemine 2.8 molecules per nm^2 (taking the average molar mass of alkoxyamines), and EPR measurment reports a concentration of 2-6 *10 $^{-7}$ M. Using the AAS data and loading established by EA , it can be conlcuded the perfect covergence with EPR data.

Comparison of basic paramaters of **Au-SG$_1$**, **Au-TEMPO** and **Au-SG$_1$-TEMPO** (Fig. S2,3,4f) does not demonstrate the considerable difference in the basic paramaters descirbed in Fig. S2-4, all deviation are with the one order of measured. The broadening of plasmonic peak of AuNPs appear to be alsmot identical, so these parameters (probable agglomeration and scattering of AuNPs, amount of grafted alkoxyamine) can be neglected for the evaluation of plasmonic behaviour.

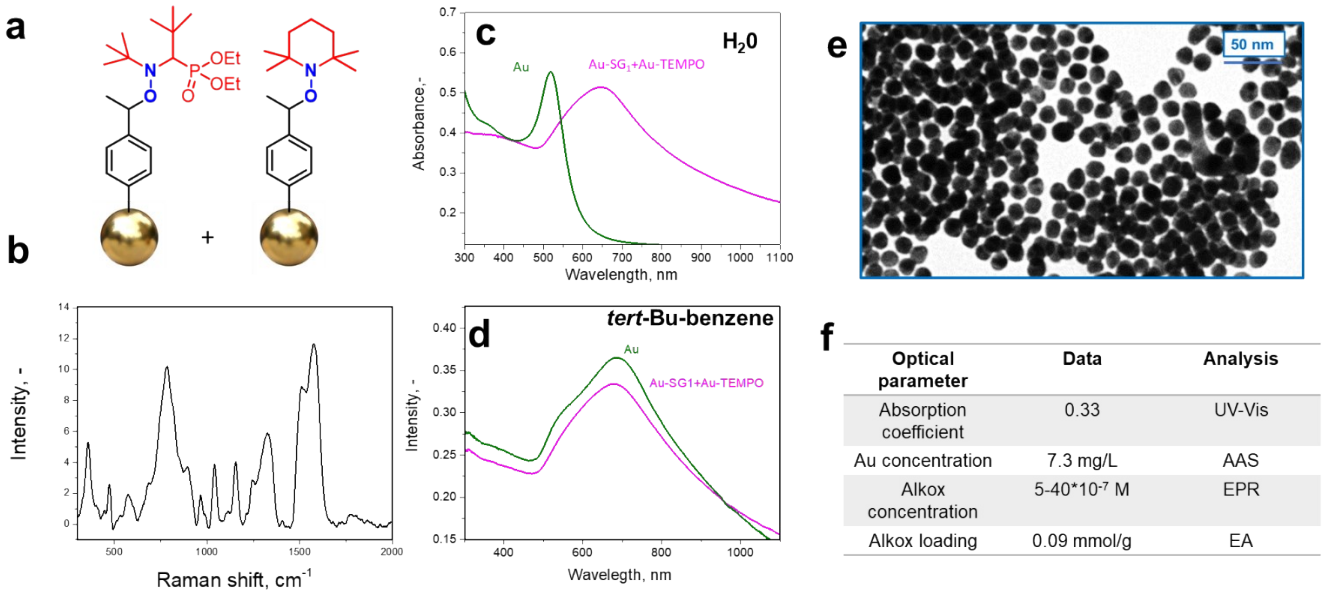

f

Optical parameter	Data	Analysis
Absorption coefficient	0.33	UV-Vis
Au concentration	7.3 mg/L	AAS
Alkox concentration	5-40*10^{-7} M	EPR
Alkox loading	0.09 mmol/g	EA

Figure S5. Detailed characterization of **Au-SG$_1$+Au-TEMPO** (a) structure, (b) SERS spectra, (c) XPS survey spectra, (d) UV-Vis spectra in water, (e) UV-Vis spectra in tert-butylbenzene (f) TEM image, (g) Summary table of parameters

*Supplementary note 6. Characterization of **Au-SG$_1$+Au-TEMPO***

Au-SG$_1$+Au-TEMPO (Fig. S5a) were prepared by the separate preparation of Au-SG$_1$ and Au-TEMPO (starting anount of AuNPs 20 ml of each), washing and transfer to tert-butylbenzene, followed by the mixing of 1.5 ml of each Au-SG$_1$ and Au-TEMPO to the final volume 3 ml. SERS spectra (Fig. S5b) demonstrate the appearance of characteristic for alkoxyamines **(1)** and **(2)** peaks of aromatic ring, P=O stretch, C-N stretch and alkyl vibrations in the region 300 -1700 cm^{-1} (see Tab. S1 for details.). The position of peaks is almost identical as in case of separate grafting of alkoxyamines **(1)** and **(2)**. UV-Vis measurment in water demonstrate the broadening and shift of peak – maximum ≈665 nm (half with 180 nm) (Fig. S5c). Transfer of **Au-SG1+Au-TEMPO** to tert-butylbenzene lead to the apperance of wider peak on UV-Vis spectra at 705 nm (half with 240 nm) (Fig. S5d, e). We also demonstrate the basic parameter of **Au-SG$_1$+Au-TEMPO** (Fig. S5f) suspension in tert-butylbenzene utilized for the furtther EPR study - 0.2 ml was taken for the each experiment from 3 ml suspension . Absorption coefficient of suspension wqas used as a common unit used to quantify the concentration of AuNPs – 0.33. We also established the concentration of gold by atomic absorbtion spectroscopy (AAS), which was found to be 7.3 mg /L.

For the calculation of alkoxyamone loading 2 methods were used: EA, and EPR measurment – after the plateu establishment of radical release. The change in nitrogen content after modification was used to calculate the alkoxiamine loading in mmol per g of AuNPs. The elemental composition of the grafted alkox SG-1 groups allowed us to establish 0.09 mmol of functional groups per 1 g of AuNPs. EPR measurment reports a concentration of 5-40 *10 $^{-7}$ M. Using the AAS data and loading established by EA, it can be conlcuded the perfect covergence with EPR data.

Comparison of basic paramaters of **Au-SG$_1$**, **Au-TEMPO**, **Au-SG$_1$-TEMPO** and **Au-SG$_1$+Au-TEMPO** (Fig. S2-5f) does not demosntarte the considerable difference in the basic paramaters descirbed in Fig., all deviation are with the one order of measured. The broadening of plasmonic peak of AuNPs appear to be alsmot identical, so these parameters (probable agglomeration and scattering of AuNPs, amount of grafted alkoxyamine) can be neglected for the evaluation of plasmonic behaviour.

(A)

	Au	C	N	O
Au	41.5	48.2	-	10.3
Au-SG1	20.9	58.2	2.2	18.7
Au-TEMPO	24.6	55.3	2.3	17.8
Au-SG1-TEMPO	23.6	56.3	3.3	23.4

(B)

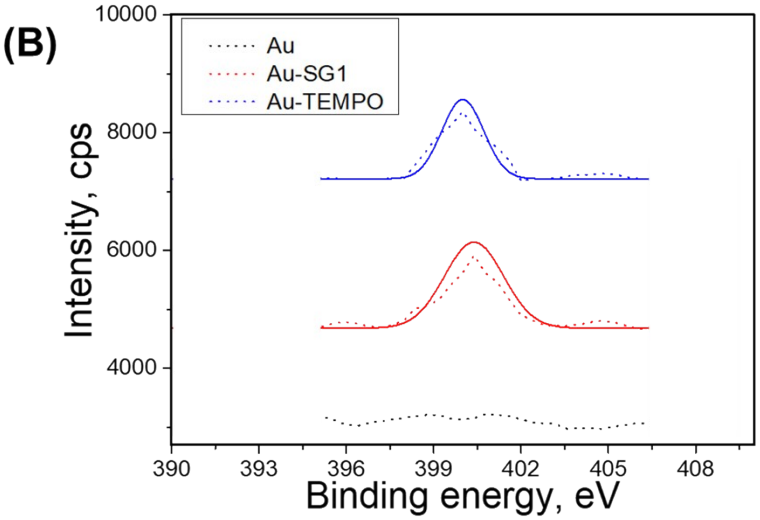

Figure S6. (A) XPS derived atomic concentration, (B) N1s region of AuNPs before and after modification with alkoxyamines **1** and **2**

Supplementary note 7. XPS -derived calculations

Calculation of organic functional groups films thickness by XPS

On the Au pristine sample, the presence of carbon and oxygen traces are visible, due to the presence of citrate [S1]. Au $4f_{7/2}$ peak of gold was used for the calculation of organic film thickness. The thickness of organic film can be estimated from the surface chemical composition and signal intensities according to [S8]. We observed gold signal (Au $4f_{7/2}$ is chosen, 85.2-88.08 eV) attenuation after modification due to attachment of functional groups and covering of surface, which can be used for calculation of organic layer thickness using following equation:

$I/I_0 = \exp(-d/\lambda \sin\theta)$

d- organic layer thickness

λ- mean free path of the substrate-specific photoelectron in the organic layer

θ- the analysis take-off angle relative to the surface (90° in our case)

I/I_0- ratio of the Au$4f_{7/2}$ peak intensities (before and after modification)

The value of λ was deduced from the empirical formula derived by Seah and Dench [S7]

$\lambda k = An/E_k^2 + BnE_k^{1/2}$, where E_k is the kinetic energy of photoelectrons.

For an Al Kα source E_k = 1486.6 – EB

If the substrate is coated with organic materials, A_n = 49 and B_n = 0.11, the unit of λ is mg*m^{-2} and the unit of energy is the electronvolt. To convert λ into nanometer units, it has to divide λ in mg*m^{-2} by the density of the overlayers, assumed here to be equal to 1.0 g/cm^3(alkoxyamines). For Au$4f_{7/2}$, λ_k is calculated to be 4.12 mg*m^{-2} and the aryl adlayer thickness is found to be:

1.8 nm for **Au-SG_1**

2.1 nm **Au-TEMPO**

1.4 nm **AuSG_1-TEMPO**

Calculation of the density of grafted alkoxyamines

The surface coverage for AuNPs grafted with SG_1 (molar weight is 399 g/mol) was . calculated according to formula (Na Avagadro number, ρ density of organic layer, d- thickness, M- molar mass):

$$\Gamma_{SG1} = \frac{Na * \rho * d}{M} = \frac{6.02 * 10^{23} * 1 * 1.8}{399 * 10^{21}} = 2.7 \frac{molecules}{nm^2}$$

For TEMPO groups, the thickness is 2.1 nm (molar weight is 216 g/mol).

$$\Gamma_{TEMPO} = \frac{Na * \rho * d}{M} = \frac{6.02 * 10^{23} * 1 * 2.1}{216 * 10^{21}} = 5.7 \frac{molecules}{nm^2}$$

For mixed alkoxyamines, the thickness is 1.4 nm (molar weight is average from both alkoxyamines 307 g/mol).

$$\Gamma_{SG1\text{-}TEMPO} = \frac{Na * \rho * d}{M} = \frac{6.02 * 10^{23} * 1 * 1.4}{307 * 10^{21}} = 2.8 \frac{molecules}{nm^2}$$

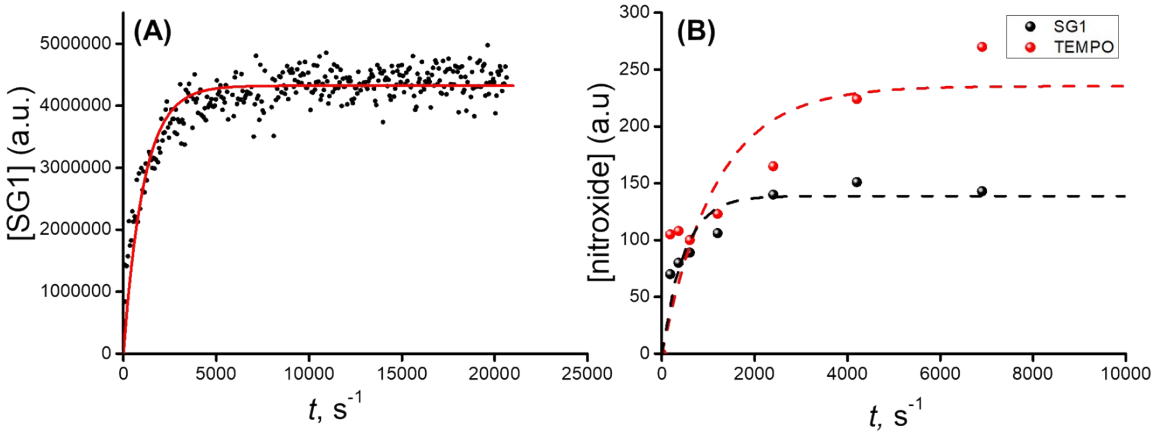

Figure S7. Kinetic curves for Au-TEMPO and Au-SG_1 (A) Growth of SG_1 concertation vs time for the homolysis of Au-SG_1 alkoxyamines (entry 1) at 90 °C. Red line is for exponential fit. (B) EPR kinetics (entry 8) of the light irradiated decomposition of Au-TEMPO and Au-SG_1. Lines are for exponential fits.

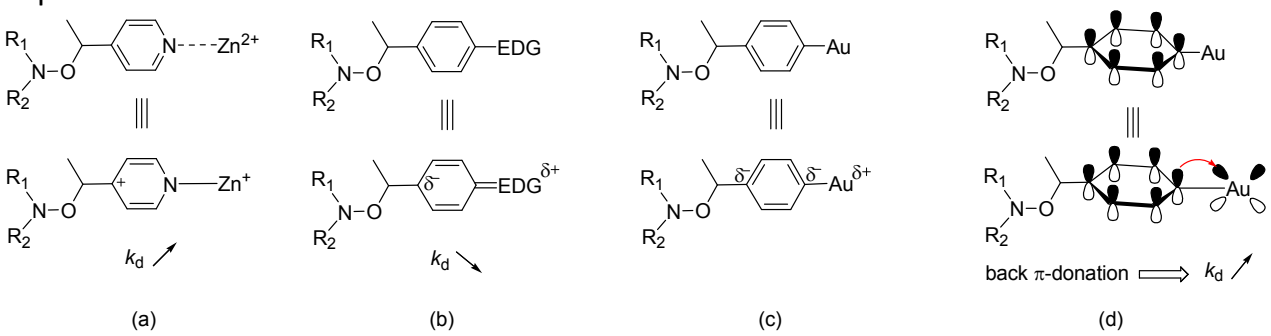

Figure S8. (a) Effect of the coordination at the *para*-position in alkoxyamines 1 and 2 by metal cation on k_d. (b) Effect of a EDG group at the *para*-position in alkoxyamines 1 and 2 on k_d. (c) Distribution of electron partial charges on the aromatic moiety of 1 and 2. (d) Back p-donation of p electron of the aromatic moiety into empty *d* or *f* orbitals of Au atom accounting for the increase in k_d.

Supplementary note 8. Electronic effect in ***Au-TEMPO/SG$_1$***

Obviously, the formation of covalent bond with electron-rich metal should also effect on the homolysis rate and k_d. Recently, it was reported that the coordination at the position *para* of pyridyl moiety of SG_1-based alkoxyamines increased k_d by a 20-fold factor [S9,S10], which can be connected with the raise of partial positive charge at the *ipso*-position affording an increase of the electronegativity π of the C-atom of the C—ON moiety and further increase in k_d (Fig. S8a) [S11]. Moreover, it is reported that the presence of EDG at the position *para* of aryl moiety of SG_1-based alkoxyamines afforded a decrease in k_d due to the raise of the partial negative charge at the *ipso* position (Fig. S8b) [S12]. Hence, a carbon-metal bond such as aryl—Au is expected to afford a strong partial negative charge at the position *para* and, then, at the position *ipso* (Fig. S8c). Therefore, a decrease in k_d should be observed for **Au-SG$_1$** in sharp contrast to the increase in k_d as observed in Table S2 (entry 4). This trend in k_d is taken into account by a back donation of π-electrons in empty *d* (as displayed in Fig. S8 as example) and *f* orbitals of Au atom favouring the raise of partial positive charge at the *ipso* position of the aryl moiety leading to the observed increase in k_d as described in Fig. S8a. As *para*-substituted TEMPO derivatives [S13] showed the same trend as SG_1-based alkoxyamines, comments done above hold for **Au-TEMPO** (entry 2 in Table S2). Hence, at 25 °C, after 3 hours at 25 °C (time after which a plateau in nitroxide concentration is reached upon LED irradiation (see Figure S3 and Fig. 6B), 0.01% and 0.3% conversion of **Au-SG$_1$** and **Au-TEMPO**, respectively, are

expected in their corresponding nitroxides, meaning that such molecules are thermally stable under our experimental conditions [S13].

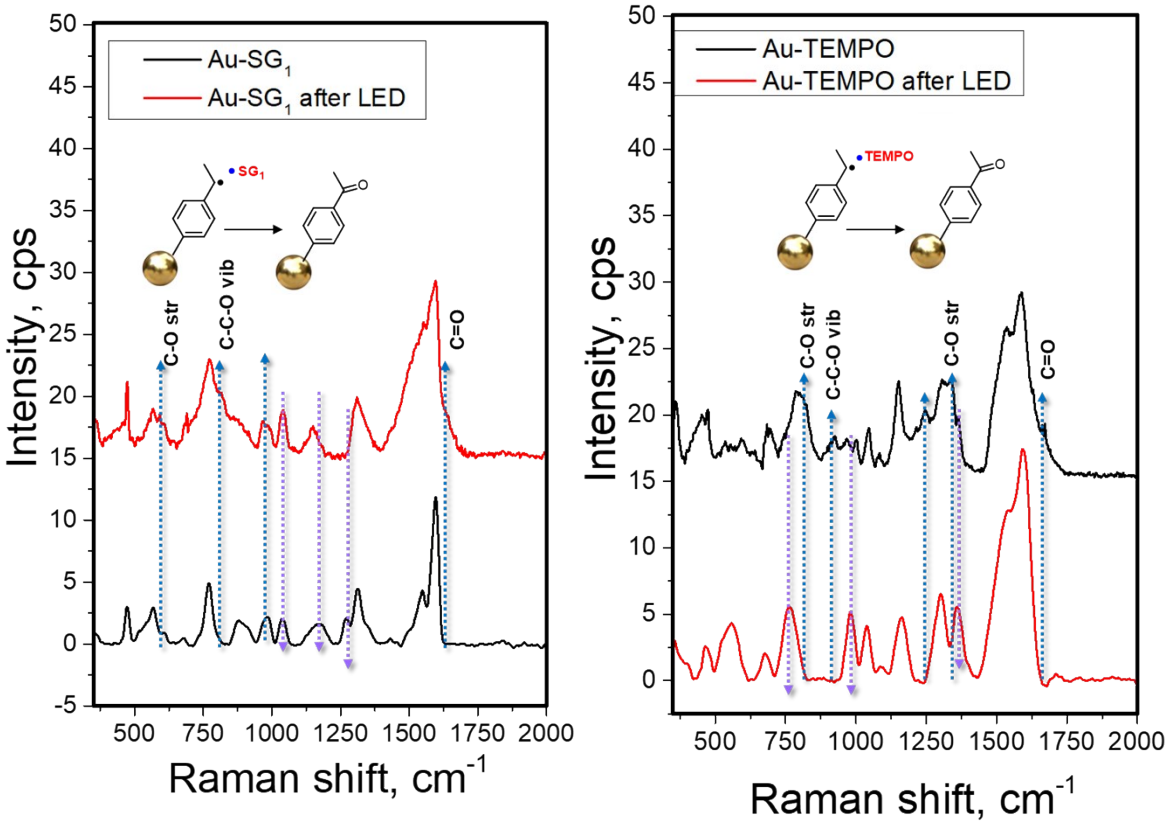

Figure S9 SERS spectra of **Au-TEMPO** and **Au-SG$_1$** before and after LED (780 nm, 7 mW/mm^2) irradiation.

*Supplementary note 9. Raman investigation of **Au-TEMPO** and **Au-SG$_1$** after plasmon-induced homolysis*

We recorded the SERS spectra of **Au-TEMPO** and **Au-SG$_1$** after the irradiation and saturation of radical evolution. AuNPs were isolated by centrifugation, washed 3 time with methanol and deposited on silicon wafers for measurements. Both SERS spectra of **Au-SG$_1$** and **Au-TEMPO** demonstrate the diminishing of peaks ascribed as N-O vibrations at 1311 and 1364 cm^{-1} due to the NO-C homolysis and detachment of generated radicals. Moreover, we observed the decrease of aliphatic peaks at 1043, 877 cm^{-1} (**Au-SG$_1$**) and 986, 760 cm^{-1} (**Au-TEMPO**). Instead of these peaks, there are a range of appeared peaks typical for the carbonyl-containing compounds. The aromatic peaks are widening with the neck at 1646-1666 cm^{-1} due to the appearance of C=O vibrations, there are also new peaks at 990, 826, 607 cm^{-1} (**Au-SG$_1$**) and 1315, 1246, 930, 814 cm^{-1} (**Au-TEMPO**) assigned to C-O and C-C-O vibrations. Therefore, we suppose that after the generation of SG$_1$ and TEMPO radical, alkoxyamines are transformed to corresponding ketone or some oxidized form.

Table S2. Overall experimental results of this work

Entry	Material	T (°C)[d]	k_d (s^{-1})[i]	E_a (kJ/mol)[h]/T_p (°C)[p]	comments	nitroxide (M)
1	**Au-SG$_1$**	90 - 120	[a]	119.4[b]/[q]	Thermal homolysis	[c]
2	**Au-SG$_1$**	25	0.00111	[q]/86	batch 1	5 10^{-7}
3	**Au-SG$_1$**	25	0.00190	[q]/91	batch 2	2 10^{-7}
4	**Au-TEMPO**	90 - 131	[e]	127.9[f]/[q]	Thermal homolysis	[g]
5	**Au-TEMPO**	25	0.00037	[q]/102	batch 1	2 10^{-7}
6	**Au-TEMPO**	25	0.00125	[q]/113	batch 2	6 10^{-7}
7	**Au-TEMPO+Au-SG$_1$**	25	0.00100[j]	[q]/86	90:10 [SG1]:[TEMPO][k,m]	4 10^{-6}
8	**Au-TEMPO+Au-SG$_1$**	25	0.00216[n] 0.00086[o]	[q]/92 [q]/110	40:60 [SG1]:[TEMPO][l,m]	5 10^{-7}
9	**Au-SG$_1$-TEMPO**	25	0.00288[n] 0.00206[o]	[q]/96 [q]/118	20:80 [SG1]:[TEMPO][m]	4 10^{-7}

[a] At 90 °C, k_d varies from 0.00092 s^{-1} to 0.0059 s^{-1} depending on the batch of NP. [b] Averaged values of all (4) measurements performed in footnote *a*. [c] Concentration in nitroxide ranging from 2 10^{-7} M to 10^{-6} M. [d] Temperature observed in the EPR cavity. [e]At 90 °C, k_d are 0.00014 s^{-1} to 0.00008 s^{-1} depending on the batch of NP. [f] Averaged values of all (4) measurements. [g] Concentration in nitroxide ranging from 2 10^{-7} M to 5 10^{-7} M. [h] Errors on E_a are assumed at 2 kJ/mol. [i] Errors on k_d are less than 10%. [j] k_d = 0.0014 s^{-1} when generation of both TEMPO and SG1 are included. [k] It was a 1:1 mixture in volume of NP suspension [l] It was a 3:2 mixture in volume of NP suspension [m] Ratio given by fitting EPR signal with Winsim 2000 sofware. Ratio is constant all along the kinetic. [n] For SG_1. [o] For TEMPO. [p] Estimated T assuming a pure thermal effect for Plasmon effect. [q] Not determined (modification with 1:1 TEMPO and SG_1 ADTs).

Supplementary note 10. Mixing two types of nanoparticles **Au-TEMPO**+**Au-SG$_1$**

To discard any side effect due to set-up and the procedure of irradiation, solutions of **Au-TEMPO** mixed with **Au-SG$_1$** are prepared and irradiated. For entry 7,8 (Table S2), solution was mainly made of **Au-TEMPO** impeding any measurements of kinetics of **Au-SG$_1$** but very close value of k_d to those of **Au-TEMPO** pure is observed. Thus, another mixture exhibiting a better ratio **Au-TEMPO** / **Au-SG$_1$** is prepared and irradiated (entry 8 in Table S2). Hence, k_d values are measured for both **Au-TEMPO** and **Au-SG$_1$**. Then, T_p values estimated are very similar to those reported for pure **Au-TEMPO** (entry 6 in Table S2) and **Au-SG$_1$** (entry 3 in Table S2), supporting again the occurrence of nonthermal plasmon effect.

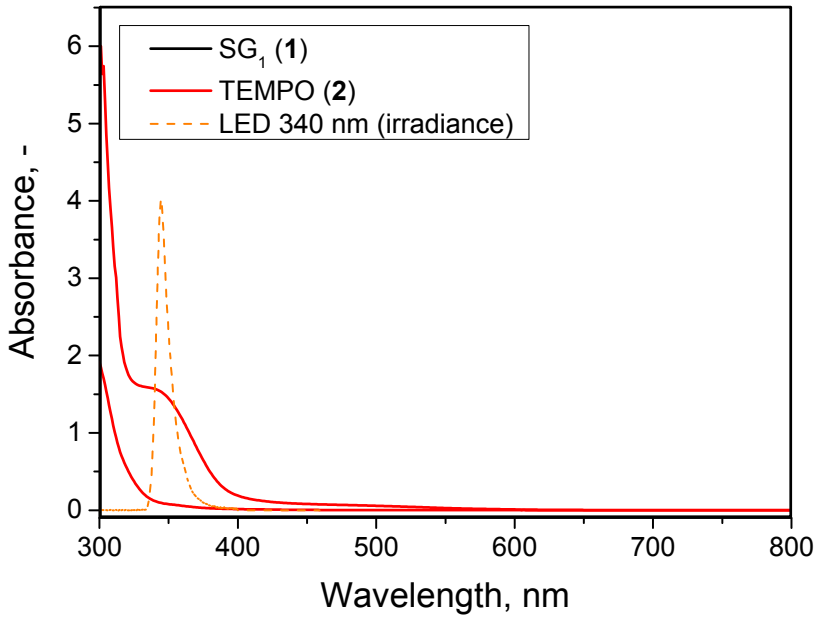

Figure S10. UV-Vis spectra of 1,2 and irradiance of LED with the wavelength 340 nm

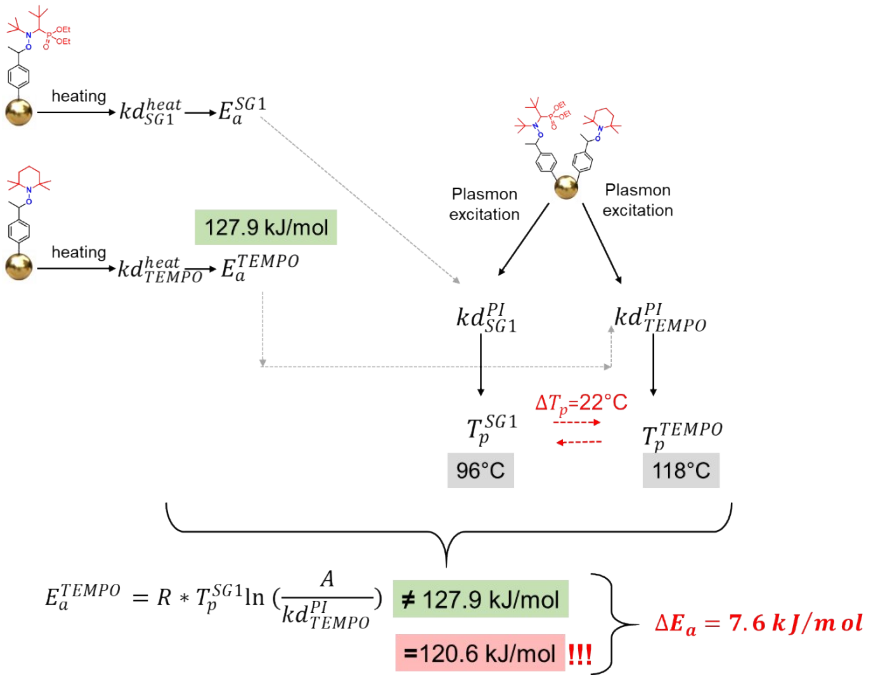

Figure S11. Schematic representation of kinetic parameters calculations

Supplementary note 11. Comparison of kinetic parameters of plasmon-assisted homolysis.

The kinetic experiments and comparison of kinetic parameters were conducted using simplified algorithm. In the first step, we determined the k_d for the thermal homolysis of **Au-TEMPO** and **Au-SG$_1$** in order to calculate the activation energy of process. Subsequent experiment of **Au-SG$_1$-TEMPO** homolysis under irradiation wit simultaneous detection of both nitroxide radicals was applied for the estimation of difference between kinetic

parameters. Thus, in this case, the kd_{SG1}^{PI} was used for the calculation of T_p^{SG1}, i.e. SG_1 moieties served as the intrinsic thermal probe. Calculation of T_p^{TEMPO} using kd_{TEMPO}^{PI} in the same process led to the 22°C difference, which revealed the contribution of non-thermal effects. For the estimation of energy associated with such contribution, we calculated the E_a^{TEMPO} using T_p^{SG1} (as a temperature determined by kinetics of intrinsic thermal probe – SG_1). The difference between activation energies was 7.6 kJ / mol.

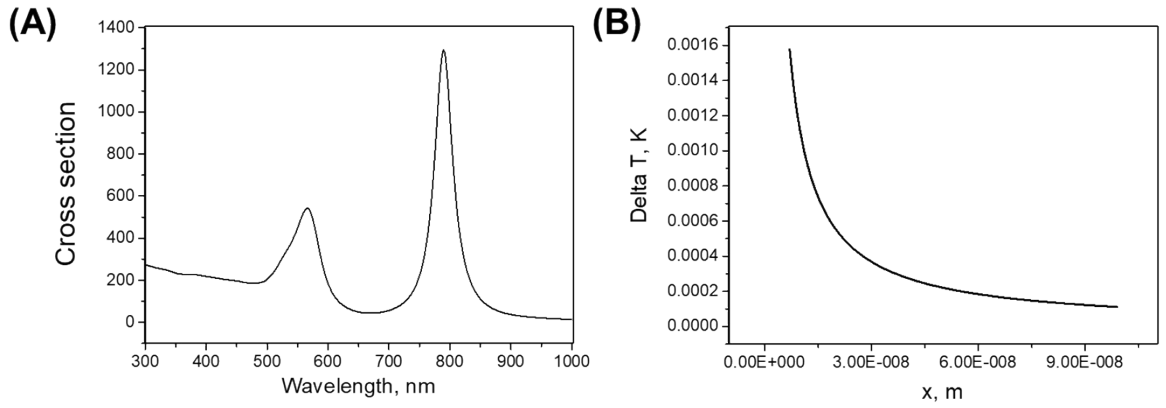

Figure S12. (A) Simulated dimer cross-sections of AuNPs (B) A curve fit of steady state temperature in Kelvins as a function of distance.

Supplementary note 12. Estimation of plasmonic local heating

Due to the aggregation of nanoparticles, which follows from the absorption peak broadening, the experimental system cannot be modeled by non-interacting particles. Thus, dimer was selected as a model system to get absorption cross-sections. The calculation was performed in the framework of Generalized Multiparticle Mie theory, implemented in the py_gmm software [S3]. Obtained cross-sections were used to calculate local heat effects on the AuNPs, under the assumption of homogeneous heat generation in the whole AuNPs volume, which is sensible due to small size and high thermal conductivity of the nanoparticle. It is important to note that cross-section of a dimer was used as if they were cross section of an isolated nanoparticle. This assumption is overoptimistic, and we use it to estimate an upper bound for the local temperature elevation. Calculation were performed according to the semi-analytical solution of the heat flow from the sphere in an infinite medium, derived by Goldenberg and Tranter [S14]. It was found that under experimental condition temperature elevation in the vicinity of nanoparticle is in the order of 10^{-3} °C, which is chemically insignificant. It is interesting to estimate the LED power density needed to achieve the local temperature elevation of 66 °C. It was found by numerically solving corresponding equation that such elevation is reached under illumination of $\sim 5.02*10^8 J/m^2$, a quantity that can be achieved only with pulsed laser and would obviously evaporate the solvent. Thus, conducted calculations clearly demonstrate that local heating effects are negligible.

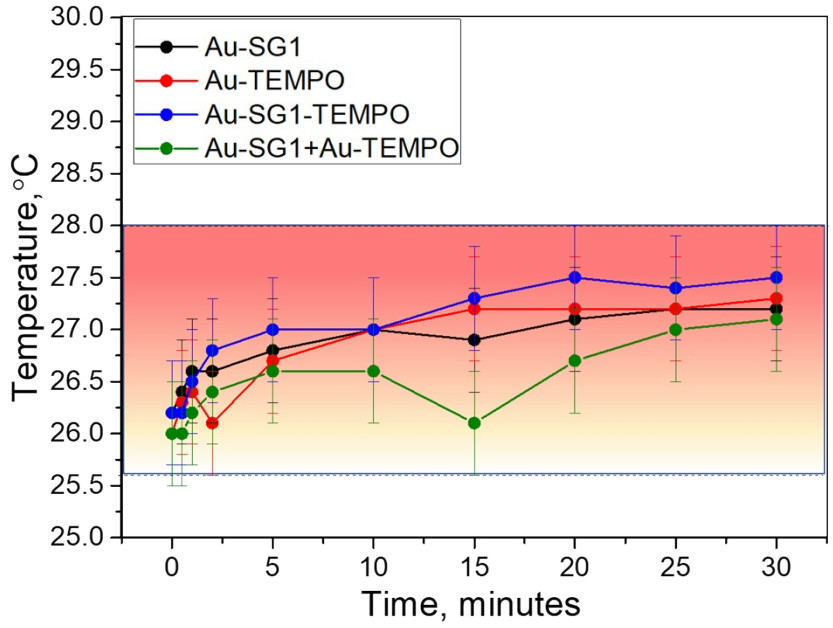

Figure S13. Monitoring of temperature of AuNPs during irradiation with LED

Supplementary note 13. Monitoring of samples temperature during plasmon-induced homolysis

The AuNPs (**Au-SG$_1$**, **Au-TEMPO**, **Au-SG$_1$-TEMPO**, **Au-SG$_1$+Au-TEMPO**) were dispersed in 5 ml tert-butylbenzene in the test tube (10 ml) with the analogues parameters to NMR tube and the ultrathin leaf-type thermocouple was placed inside the test tube, the tube was carefully sealed. LED source (780 product number M780LP1, Thorlab) was set up vertically to be the distance from LED to vial 1 cm. The spot size of LED was approximately 1 cm^2 (emitter diameter 3 mm) at this distance the power was measured nm7 mW/mm^2 by Integrating Sphere Photodiode Power Sensors (Thorlabs, S142C). The laser beam was focused on the test tube close to the working edge of the thermocouple, and temperature changes were monitored until a saturated value was reached (3 min of illumination was found to be enough for the achievement of stabilized temperature value).

References

[S1] Kimling, J.; Maier, M.; Okenve, B.; Kotaidis, V.; Ballot, H.; Plech, A. Turkevich Method for Gold Nanoparticle Synthesis Revisited. *J. Phys. Chem. B* **2006**, *110* (32), 15700–15707. https://doi.org/10.1021/jp061667w.

[S2] Audran, G.; Brémond, P.; Joly, J. P.; Marque, S. R. A.; Yamasaki, T. C-ON Bond Homolysis in Alkoxyamines. Part 12: The Effect of the Para-Substituent in the 1-Phenylethyl Fragment. *Org. Biomol. Chem.* **2016**, *14* (14), 3574–3583. https://doi.org/10.1039/c6ob00384b.

[S3] Pellegrini, G.; Mattei, G.; Bello, V.; Mazzoldi, P. Interacting Metal Nanoparticles: Optical Properties from Nanoparticle Dimers to Core-Satellite Systems. *Mater. Sci. Eng. C* **2007**, *27* (5-8 SPEC. ISS.), 1347–1350. https://doi.org/10.1016/j.msec.2006.07.025.

[S4] Guselnikova, O.; Marque, S. R. A.; Tretyakov, E. V.; Mares, D.; Jerabek, V.; Audran, G.; Joly, J. P.; Trusova, M.; Svorcik, V.; Lyutakov, O.; et al. Unprecedented Plasmon-Induced Nitroxide-Mediated Polymerization (PI-NMP): A Method for Preparation of Functional Surfaces. *J. Mater. Chem. A* **2019**, *7* (20), 12414–12419. https://doi.org/10.1039/c9ta01630a.

[S5] Guselnikova, O.; Postnikov, P.; Marque, S. R. A.; Švorčík, V.; Lyutakov, O. Beyond Common Analytical Limits of Radicals Detection Using the Functional SERS Substrates. *Sensors Actuators, B Chem.* **2019**, *300*, 127015. https://doi.org/10.1016/j.snb.2019.127015.

[S6] Romero, I.; Aizpurua, J.; Bryant, G. W.; García De Abajo, F. J. Plasmons in Nearly Touching Metallic Nanoparticles: Singular Response in the Limit of Touching Dimers. *Opt. Express* **2006**, *14* (21), 9988. https://doi.org/10.1364/oe.14.009988.

[S7] Pellegrini, G.; Mattei, G.; Bello, V.; Mazzoldi, P. Interacting Metal Nanoparticles: Optical Properties from Nanoparticle Dimers to Core-Satellite Systems. *Mater. Sci. Eng. C* **2007**, *27* (5-8 SPEC. ISS.), 1347–1350. https://doi.org/10.1016/j.msec.2006.07.025.

[S8] Schumacher, L.; Jose, J.; Janoschka, D.; Dreher, P.; Davis, T. J.; Ligges, M.; Li, R.; Mo, M.; Park, S.; Shen, X.; et al. Precision Plasmonics with Monomers and Dimers of Spherical Gold Nanoparticles: Nonequilibrium Dynamics at the Time and Space Limits. *J. Phys. Chem. C* **2019**, *123* (21), 13181–13191. https://doi.org/10.1021/acs.jpcc.9b01007.

[S9] Audran, G.; Bagryanskaya, E.; Bagryanskaya, I.; Brémond, P.; Edeleva, M.; Marque, S. R. A.; Parkhomenko, D.; Tretyakov, E.; Zhivetyeva, S. C-ON Bond Homolysis of Alkoxyamines Triggered by Paramagnetic Copper(II) Salts. *Inorg. Chem. Front.* **2016**, *3* (11), 1464–1472. https://doi.org/10.1039/c6qi00277c.

[S10] Audran, G.; Bagryanskaya, E.; Bagryanskaya, I.; Edeleva, M.; Joly, J. P.; Marque, S. R. A.; Iurchenkova, A.; Kaletina, P.; Cherkasov, S.; Hai, T. T.; et al. How Intramolecular Coordination Bonding (ICB) Controls the Homolysis of the C-ON Bond in Alkoxyamines. *RSC Adv.* **2019**, *9* (44), 25776–25789. https://doi.org/10.1039/c9ra05334d.

[S11] Brémond, P.; Marque, S. R. A. First Proton Triggered C-ON Bond Homolysis in Alkoxyamines. *Chem. Commun.* **2011**, *47* (14), 4291–4293. https://doi.org/10.1039/c0cc05637e.

[S12] Yamasaki, T.; Buric, D.; Chacon, C.; Audran, G.; Braguer, D.; Marque, S. R. A.; Carré, M.; Brémond, P. Chemical Modifications of Imidazole-Containing Alkoxyamines Increase C–ON Bond Homolysis Rate: Effects on Their Cytotoxic Properties in Glioblastoma Cells. *Bioorganic Med. Chem.* **2019**, *27* (10), 1942–1951. https://doi.org/10.1016/j.bmc.2019.03.029.

[S13] Marque, S.; Fischer, H.; Baier, E.; Studer, A. Factors Influencing the C-O Bond Homolysis of Alkoxyamines: Effects of H-Bonding and Polar Substituents. *J. Org. Chem.* **2001**, *66* (4), 1146–1156. https://doi.org/10.1021/jo001190z.

[S14] Goldenberg, H.; Tranter, C. J. Heat Flow in an Infinite Medium Heated by a Sphere. *Br. J. Appl. Phys.* **1952**, *3* (9), 296. https://doi.org/10.1088/0508-3443/3/9/307.